

Circulation Research

JOURNAL OF THE AMERICAN HEART ASSOCIATION



Regulation of Oxygen Distribution in Tissues by Endothelial Nitric Oxide

Victor M. Victor, Cristina Nuñez, Pilar D'Ocón, Cormac T. Taylor, Juan V. Esplugues and Salvador Moncada

Circ. Res. 2009;104;1178-1183; originally published online Apr 30, 2009;

DOI: 10.1161/CIRCRESAHA.109.197228

Circulation Research is published by the American Heart Association, 7272 Greenville Avenue, Dallas, TX 75214

Copyright © 2009 American Heart Association. All rights reserved. Print ISSN: 0009-7330. Online ISSN: 1524-4571

The online version of this article, along with updated information and services, is located on the World Wide Web at:

<http://circres.ahajournals.org/cgi/content/full/104/10/1178>

Data Supplement (unedited) at:

<http://circres.ahajournals.org/cgi/content/full/CIRCRESAHA.109.197228/DC1>

Subscriptions: Information about subscribing to Circulation Research is online at
<http://circres.ahajournals.org/subscriptions/>

Permissions: Permissions & Rights Desk, Lippincott Williams & Wilkins, a division of Wolters Kluwer Health, 351 West Camden Street, Baltimore, MD 21202-2436. Phone: 410-528-4050. Fax: 410-528-8550. E-mail:
journalpermissions@lww.com

Reprints: Information about reprints can be found online at
<http://www.lww.com/reprints>

Regulation of Oxygen Distribution in Tissues by Endothelial Nitric Oxide

Victor M. Victor, Cristina Nuñez, Pilar D'Ocón, Cormac T. Taylor,
Juan V. Esplugues,* Salvador Moncada*

Abstract—Nitric oxide (NO) decreases cellular oxygen (O₂) consumption by competitively inhibiting cytochrome *c* oxidase. Here, we show that endogenously released endothelial NO, either basal or stimulated, can modulate O₂ consumption both throughout the thickness of conductance vessels and in the microcirculation. Furthermore, we have shown that such modulation regulates O₂ distribution to the surrounding tissues. We have demonstrated these effects by measuring O₂ consumption in blood vessels in a hypoxic chamber and O₂ distribution in the microcirculation using the fluorescent oxygen-probe Ru(phen)₃²⁺. Removal of NO by physical or pharmacological means, or in eNOS^{-/-} mice, abolishes this regulatory mechanism. Our results indicate that, in addition to its well-known effect on the regulation of vascular tone, endothelial NO plays a major role in facilitating the distribution of O₂, an action which is crucial for the adaptation of tissues, including the vessel wall itself, to hypoxia. It is possible that changes in the distribution of O₂ throughout the vessel wall may be implicated in the origin of vascular pathologies such as atherosclerosis. (*Circ Res.* 2009;104:1178-1183.)

Key Words: nitric oxide ■ endothelium ■ oxygen consumption

Nitric oxide (NO) synthase in the vasculature (endothelial NO synthase [eNOS]) is constantly activated by the shear stress generated by circulating blood. The resulting NO, which activates soluble guanylate cyclase (sGC), maintains a vasodilator tone which is determinant in the regulation of blood flow and pressure.¹ NO also interacts with the terminal enzyme of the electron transport chain, cytochrome *c* oxidase (CcO), in a manner that is competitive with oxygen (O₂), leading to an increase in the *K_m* of this enzyme for O₂ and the consequent inhibition of respiration.² A number of studies in vascular endothelial cells³ and in tissues^{4,5} have shown that this results in a decrease in consumption of O₂ and in its redistribution away from mitochondria and toward other oxygen-dependent targets.⁶ Thus NO plays a role in the subcellular profile of O₂ distribution. In this study, we have investigated this phenomenon by monitoring the dynamics of O₂ consumption and its distribution both in a variety of strips of conductance vessels from several species and in the mesenteric circulation of rats and mice. Our results indicate that NO plays a major role in facilitating O₂ distribution in these vascular tissues through its effect as an inhibitor of the mitochondrial CcO. This action, which increases as the O₂ concentration [O₂] decreases, might be a major factor in the adaptation of tissues to hypoxia.

Materials and Methods

Tissue Preparation

Human umbilical cords were obtained from the Department of Gynaecology and Obstetrics of the Hospital Doctor Peset. Vascular rings, 5 mm in length, were extracted from the middle portion of the cords. Male Sprague-Dawley rats (200 to 250 g, Harlan Laboratories, Barcelona, Spain) or wild-type (WT) and eNOS knockout (eNOS^{-/-}) mice (WT, C57BL/6Jx129, 20 to 25 g, UCL, London, UK) were decapitated and their thoracic aortas and pulmonary and mesenteric arteries were removed, cleaned of adhering tissues, and cut into 5-mm (rat vessels) or 2-mm (mouse vessels) rings. When necessary, the endothelium was disrupted by gently rubbing the luminal surface. For the experiments with fluorescence microscopy, a portion of the rat or mouse mesenteric arterial tree was isolated and cleaned of surrounding fat. All experiments were performed in Krebs solution (in 10⁻³ mol/L) (NaCl 118, KCl 4.75, CaCl₂ 1.9, MgSO₄ 1.2, KH₂PO₄ 1.2, NaHCO₃ 25, and glucose 10.1). All protocols complied with the European Community guidelines for the use of experimental animals and were approved by the Ethics Committee of the University of Valencia.

Contractility Studies

These experiments were performed with rat vascular rings suspended in a 5-mL organ bath (37°C) gassed with 12% O₂, 5% CO₂, and 83% N₂, which produced an O₂ concentration of ≈130×10⁻⁶ mol/L, similar to that present in the aortic blood,^{7,8} and monitored with a dissolved O₂ meter (ISO₂; World Precision Instruments, Stevenage, Herts, UK). Tension was measured isometrically with Grass FTO3

Original received October 15, 2008; resubmission received March 16, 2009; revised resubmission received April 20, 2009; accepted April 20, 2009. From the Fundación Hospital Universitario Doctor Peset (V.M.V.), Valencia, Spain; Departamento de Farmacología and CIBERehd (V.M.V., C.N., P.D., J.V.E.), Facultad de Medicina, Universidad de Valencia, Spain; University College Dublin Conway Institute (C.T.T.), Ireland; and Wolfson Institute for Biomedical Research (S.M.), University College London, United Kingdom.

*Both authors contributed equally to this work.

Correspondence to Prof S. Moncada, The Wolfson Institute for Biomedical Research, University College London, Gower St, London WC1E 6BT, United Kingdom. E-mail s.moncada@ucl.ac.uk

© 2009 American Heart Association, Inc.

Circulation Research is available at <http://circres.ahajournals.org>

DOI: 10.1161/CIRCRESAHA.109.197228

force-displacement transducers and recorded (Power Laboratory). An initial load of 2 g (aorta and human umbilical artery) or 1 g (pulmonary and mesenteric arteries) was applied to each preparation and maintained throughout the experiment. Following a 75- to 90-minute equilibration period, rings were contracted with phenylephrine (Phe) (1×10^{-5} mol/L in mesenteric artery or 1×10^{-6} mol/L in pulmonary artery, aorta, and human umbilical artery), and the presence of a functional endothelium was confirmed by eliciting a relaxant response (>95%) to acetylcholine (ACh) (1×10^{-5} mol/L), a dose that induces maximal sGC-mediated vasodilatation.⁷

After a further equilibration period of 30 to 45 minutes, vessels were contracted with a depolarizing solution (60×10^{-3} mol/L KCl) to obtain the maximal level of contraction. After further washing, the rings were allowed to equilibrate for at least 1 hour. Thereafter, they were again stimulated with Phe and concentration-response curves of relaxation to ACh (1×10^{-9} to 1×10^{-5} mol/L), bradykinin (Bk) (1×10^{-9} to 1×10^{-5} mol/L), or the slow-releasing NO donor diethylenetriamine (DETA-NO) (1×10^{-8} to 1×10^{-4} mol/L) were carried out. In another set of experiments concentration-response curves of contraction to Phe (1×10^{-10} to 10×10^{-6} mol/L) were performed. The concentration ($-\log[\text{mol/L}]$) that produced 95% of the maximal effect (pEC_{95}) was obtained by a nonlinear regression analysis with GraphPad software.

Electrochemical Measurement of O₂ Consumption

Aortic rings from 2 rats (80 to 100 mg total wet weight) or 3 mice (20 to 30 mg wet weight), pulmonary and mesenteric rings from 3 rats (15 to 25 mg wet weight), or human umbilical arteries (190 ± 5 mg total wet weight) were placed in gas-tight chambers containing 1 mL of Krebs solution and gently agitated at 37°C. The O₂ consumption by the tissue was measured with a Clark-type O₂ electrode (Rank Brothers, Bottisham, UK) calibrated with an air-saturated Krebs solution, assuming an [O₂] of 200×10^{-6} mol/L. Experiments were performed in the presence of the NO synthase inhibitor N^ω-nitro-L-arginine (L-NA) (1×10^{-4} mol/L), the sGC inhibitor 1*H*-1,2,4-oxadiazolo[4,3-*a*]quinoxalin-1-one (ODQ), (5×10^{-6} mol/L), ACh (1×10^{-5} mol/L), Bk (1×10^{-5} mol/L), or Phe (1×10^{-5} mol/L in mesenteric artery or 1×10^{-6} mol/L in pulmonary artery, aorta, and human umbilical artery) in intact or endothelium-denuded vessels. Sodium cyanide (1×10^{-3} mol/L) was used to confirm that O₂ consumption was mainly mitochondrial ($\approx 95\%$ to 99%). In some experiments, the reversibility of NO-induced inhibition of respiration was assessed by adding oxyHb (1×10^{-5} mol/L) when the [O₂] in the chamber was 100×10^{-6} mol/L. Measurements were obtained using a data acquisition device, Duo18 (World Precision Instruments, Stevenage, UK). A hyperbolic function was used to describe the relationship between [O₂] and the rate of O₂ consumption (VO_2).^{7,9,10} The apparent O₂ affinity (Michaelis-Menten constant [K_m]) (1×10^{-6} mol/L) was calculated using the program GraphPad, and the results are shown in the Table. VO_2 was calculated at 2 specific [O₂], 130×10^{-6} mol/L and 30×10^{-6} mol/L, which were selected as representing those [O₂] present in arterial blood or within tissues, respectively.^{7,8} VO_2 was expressed as 1×10^{-9} mol/L O₂/min per milligram of protein. Proteins were determined by the BCA protein assay kit (Pierce, Rockford, Ill) using BSA as the standard.

In some cases, the viability of the rings was later assessed by confirming that their contractile response to Phe and their relaxant response to ACh did not differ from that of nonmanipulated vessels.

Visualization of Intracellular O₂ by Fluorescence Microscopy

Selected portions ($\approx 1.5 \times 1.5$ cm) of the mesenteric arterial tree close to the gut were excised and incubated in the dark (3 hours) in Krebs solution (37°C) containing Tris(1,10-phenanthroline)ruthenium(II) chloride hydrate [Ru(phen)₃²⁺] (1×10^{-4} mol/L). This fluorochrome has recently been adapted for use as an indicator of O₂ tension in cells and tissues, where its fluorescence is inversely proportional to the concentration of O₂.^{11,12} Ruthenium-based oxygen-sensing probes sense O₂ in the range of 0 to 9.1 ppm at 20°C, although their sensitivity range in tissues may differ at 37°C.¹³ In addition to its

Table. Effect of NO on the Apparent K_m for O₂ in Rings From Rat and Human Vessels

	Rat Arteries			Human Umbilical Artery
	Aorta	Pulmonary	Mesenteric	
Control	23.2±1.3	20.7±3.1	29.3±3.1	28.6±1.8
L-NA	7.3±0.4*	10.9±1.0*	12.5±1.8*	10.1±0.8*
+E(-)	8.3±0.6*	9.9±0.7*	12.9±1.2*	6.9±0.5*
+ODQ	24.5±1.2	22.8±1.7	30.8±2.9	31.3±1.3
ACh	75.9±2.6*	42.7±2.3*	76.6±10.6*	49.4±2.6*
+L-NA	7.6±0.4*	8.3±0.2*	11.6±1.3*	9.3±0.5*
+E(-)	8.9±0.4*	7.9±0.1*	10.9±1.2*	8.4±0.6*
Bk	79.7±3.8*	46.4±2.8*	72.3±10.5*	50.6±6.3*
+L-NA	8.3±0.5*	8.1±0.3*	12.6±1.3*	9.1±0.4*
+E(-)	8.5±0.5*	9.2±0.2*	11.7±1.1*	8.7±0.3*
DETA	113.1±5.8*	78.3±5.2*	83.4±6.1*	72.5±4.4*
+L-NA	93.8±2.6*	69.4±4.1*	78.5±5.1*	68.4±6.1*
+E(-)	83.1±2.4*	66.5±5.3*	75.3±6.5*	65.6±8.1*
Phe	71.6±3.1*	38.1±3.6*	56.5±5.1*	42.2±5.1*
+L-NA	6.6±0.5*	8.3±0.5*	9.3±0.4*	10.3±5.2*
+E(-)	7.8±0.5*	7.6±0.6*	9.9±0.6*	9.6±0.5*

Samples were in treated with ACh (1×10^{-5} mol/L), Bk (1×10^{-5} mol/L), DETA-NO (1×10^{-5} mol/L), and Phe (1×10^{-5} mol/L in mesenteric artery or 1×10^{-6} mol/L in pulmonary artery, aorta, and human umbilical artery). In some cases, L-NA was added or the endothelium was removed [E(-)]. Data are means±SEM of 5–7 independent experiments. * $P < 0.05$ vs control.

strong visible absorption, efficient fluorescence, and relatively long-lived excited state, Ru(phen)₃²⁺ exhibits high O₂ sensitivity, a large Stoke shift, and high photo-/chemical stability in the cellular environment. Because of its long emission wavelength the fluorescence signal of the indicator is shifted away from cellular autofluorescence, which causes serious perturbation when UV sensing indicators are used. In our experimental conditions, ruthenium is taken up by living cells and maintains its O₂-sensing properties for at least 5 hours after loading.

The vital cell nuclear stain Hoechst 33342 (1×10^{-6} mol/L) was added for the last 30 minutes of incubation. Samples of mesentery between 2 vessel branches were then mounted on a purpose-built support and transferred to a hypoxic incubator and maintained at 37°C. This system was then placed under a fluorescence microscope (Axiovert 200M Zeiss inverted). Following equilibration for 10 minutes at atmospheric [O₂] (200×10^{-6} mol/L O₂; the O₂ concentration in the tissue medium, however, was 130×10^{-6} mol/L, as monitored with a dissolved O₂ meter [ISO₂; World Precision Instruments, Stevenage, Herts, UK]), samples were subjected to hypoxia (15×10^{-6} mol/L O₂) for 20 minutes by the addition of nitrogen in the presence or absence of the NO synthase inhibitor L-NA (1×10^{-4} mol/L), ACh (1×10^{-5} mol/L), or DETA-NO (1×10^{-5} mol/L). Images ($\times 10$ magnification) were obtained every 2 minutes throughout the entire experimental period, and changes in Ru(phen)₃²⁺ fluorescence were analyzed using a 543-nm He-Ne laser to excite the probe. A 405-nm diode laser was used to excite Hoechst 33342. Fluorescence was detected through 440/20 BP and 604 LP filters for Hoechst 33342 and Ru(phen)₃²⁺, respectively, and the fluorescence microscope settings were adjusted to produce the optimum signal to noise ratio and maximum signal detection. An analysis of the ruthenium fluorescence in individual cells was obtained with Leica image analysis software that processed the image stacks acquired in the region of interest. The ratio of fluorescence intensity was calculated for each cell using imaging software (Leica Confocal Software, version 2.61, Leica Microsys-

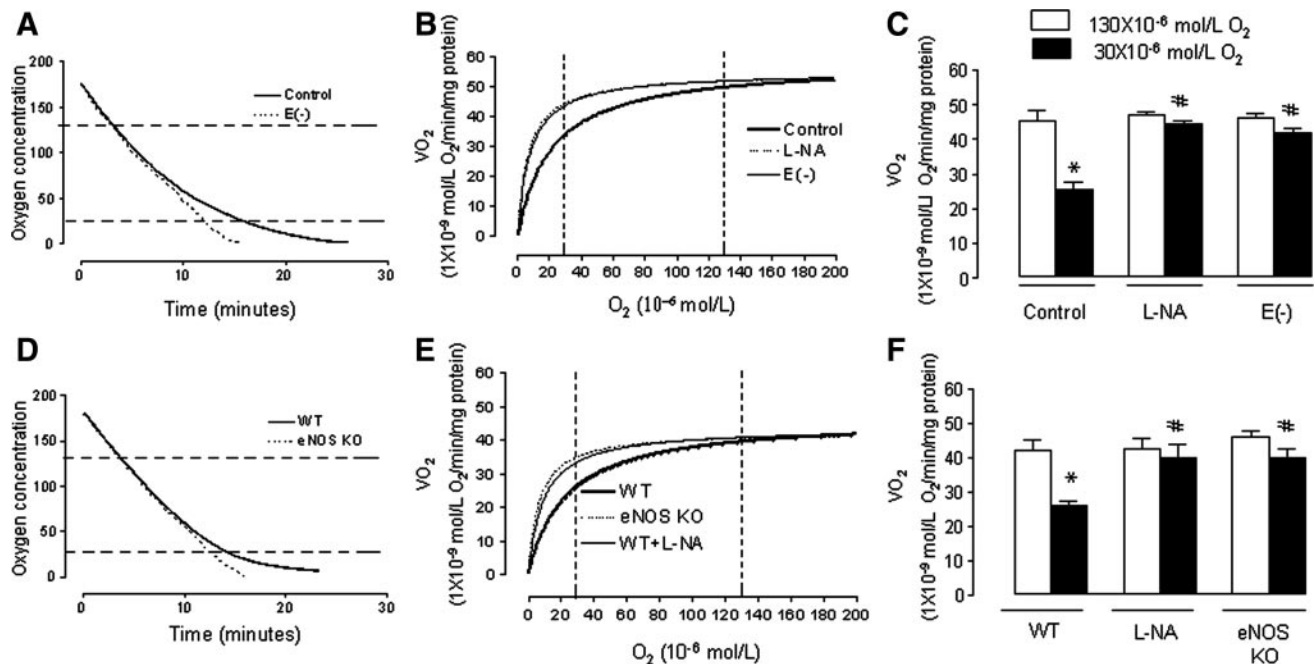


Figure 1. Representative traces showing O_2 consumption and VO_2 in rings of rat (A and B) and mouse aorta from WT and eNOS KO mice (D and E). B and E show the continuous measurement of VO_2 in the absence or presence of L-NA (1×10^{-4} mol/L) in endothelium-denuded vessels (E-) and in eNOS KO mice. VO_2 measured at 130×10^{-6} mol/L and 30×10^{-6} mol/L O_2 are shown in C and F. Data are means \pm SEM from $n \geq 5$ independent experiments, with $*P < 0.05$ vs corresponding value at 130×10^{-6} mol/L O_2 and $\#P < 0.05$ vs control value at 30×10^{-6} mol/L O_2 .

tems GmbH, Heidelberg, Germany). At least 70 cells were analyzed for each sample.

Further experiments were performed to exclude interference with $Ru(phen)_3^{2+}$ fluorescence by free radicals (H_2O_2) and NO (DETA-NO). Different concentrations (1×10^{-9} mol/L to 1×10^{-4} mol/L) of H_2O_2 and DETA-NO were incubated in the presence of $Ru(phen)_3^{2+}$ (1×10^{-4} mol/L) in a cell-free Krebs solution. Fluorescence was measured with a Fluoroskan plate reader (Thermo LabSystems). Basal fluorescence was not modified by incubation with DETA-NO or H_2O_2 , or either of the compounds in normoxia and hypoxia, except at a maximal concentration of H_2O_2 (1×10^{-4} mol/L) ($n = 4$ to 5 experiments; results not shown).

Data Analysis

Unless otherwise stated, all results are the means \pm SEM of at least 5 experiments from different animals. Statistical analysis was performed by 1-way ANOVA (GraphPad Software) and Student–Newman–Keuls as a post hoc test. Significance was defined as $P < 0.05$.

Drugs and Solutions

Phe, ACh, Bk, L-NA, sodium cyanide, ODQ, meth(a)emoglobin, $Ru(phen)_3^{2+}$, and Hoechst 33342 were acquired from Sigma-Aldrich (St Louis, Mo). DETA-NO was from Alexis (Lausen, Switzerland). OxyHb was prepared by reduction of human meth(a)emoglobin with a 10-fold molar excess of sodium dithionite, followed by dialysis against PBS. All drugs were dissolved in ultrapure water. $Ru(phen)_3^{2+}$ and Hoechst 33342 were dissolved in Krebs solution and ODQ was dissolved in DMSO (1:5000 vol:vol).

Results

Consumption of O_2 by Blood Vessels

First we monitored VO_2 in several isolated blood vessels when placed in an O_2 -tight chamber, as previously described.^{7,9,10} Figure 1A and 1B show how the rat aorta gradually reduced its rate of O_2 consumption as the $[O_2]$

decreased. The requirement of the tissue for O_2 was mainly mitochondrial because addition of sodium cyanide resulted in almost complete (95% to 99%) inhibition of O_2 consumption (data not shown). The reduction in the rate of consumption at low $[O_2]$ was attenuated both by blocking NO synthesis with L-NA and by removal of the endothelium, indicating that NO was responsible for this effect and therefore for the observed increase in the apparent K_m for O_2 (Figure 1B and the Table). This action of NO was independent of an effect on sGC because it was unaffected by treatment with the specific sGC inhibitor ODQ (Table).

Figure 1C shows the consumption of O_2 at 2 specific $[O_2]$ that approximate to those of arterial blood (130×10^{-6} mol/L) and tissue (30×10^{-6} mol/L), respectively.^{7,8} Aortas were found to consume $\approx 50\%$ less O_2 at the lower of the 2 $[O_2]$. This NO-dependent adaptive response was not observed only in the aorta but in all the vessels studied, independent of species (human, rat, mouse) or anatomic origin (placental, systemic, or pulmonary circulation) (Table).

In aortas from eNOS knockout mice, we observed a reduced apparent K_m for O_2 and similar rates of O_2 consumption at the high and low $[O_2]$ studied. This contrasted with the response of tissues from WT mice, which was similar to that of control rat aortas. The responses of tissues from the eNOS knockout mice were similar to those exhibited by WT controls after treatment with L-NA or endothelium denudation (Figure 1D through 1F).

Treatment of rat arteries with vasodilators such ACh (1×10^{-5} mol/L) or Bk (1×10^{-5} mol/L) (EC_{95}) (see Materials and Methods) that stimulate endothelial NO generation resulted in a greater inhibition of O_2 consumption at the low $[O_2]$ and, in addition, an inhibition of O_2 consumption at the

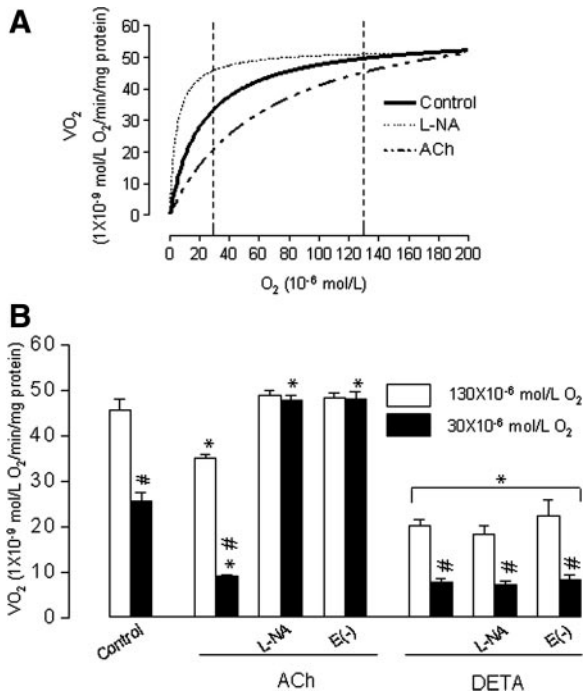


Figure 2. Effect of ACh and DETA-NO on VO_2 in rat aorta. Vessels were treated with ACh (1×10^{-5} mol/L) or DETA-NO (1×10^{-5} mol/L) in endothelium-denuded vessels (E-) or following incubation with L-NA (1×10^{-4} mol/L). A shows the continuous measurement of VO_2 , and B shows the VO_2 measured at 130×10^{-6} mol/L and 30×10^{-6} mol/L O_2 . Data are means \pm SEM from $n \geq 4$ independent experiments, with $*P < 0.05$ vs control at the corresponding O_2 , and $\#P < 0.05$ vs the corresponding value at 130×10^{-6} mol/L O_2 .

higher $[O_2]$ (Figure 2A and 2B and the Table). This did not occur when the tissues were treated with L-NA or were endothelium-denuded (Figure 2B). Unlike ACh or Bk, the greater inhibition of O_2 consumption and the increase in the K_m values induced by the slow-releasing NO donor DETA-NO (1×10^{-5} mol/L) were not significantly affected either by inhibition of NO production or by removal of the endothelium (Figure 2B). The fact that the potent vasoconstrictor Phe (EC_{95}) (1×10^{-5} mol/L in mesenteric artery or 1×10^{-6} mol/L in pulmonary artery, aorta and human umbilical artery) also induced an NO-dependent decrease in the vascular consumption of O_2 (Table) ruled out the possibility that the action of ACh, Bk, and DETA-NO was attributable to their vasodilator properties.

Concentration of O_2 in Vascular Tissue

We used the O_2 probe $Ru(phen)_3^{2+}$ (1×10^{-4} mol/L) to monitor O_2 concentrations under normal and hypoxic conditions in ex vivo portions of rat mesenteric tissue containing at least one blood vessel of ≈ 20 to $30 \mu m$ in diameter. The tissue was placed on a purpose-built support inside a chamber and analyzed under a fluorescence microscope in continuously regulated conditions of temperature ($37^\circ C$) and gas (5% CO_2 and variable concentrations of O_2), and images were obtained every 2 minutes. Following equilibration at 200×10^{-6} mol/L O_2 for 10 minutes, samples were subjected to hypoxia ($\approx 15 \times 10^{-6}$ mol/L O_2) for 20 minutes by the addition of nitrogen. As shown in Figure 3A and 3B and the

Movies and Figure I in the online data supplement (available at <http://circres.ahajournals.org>), in control experiments, this produced a rapid build up in the concentration of O_2 in the individual cells, as shown by a decrease in red fluorescence in their cytosol. This was not attributable to photobleaching by the camera because there was no change in the number of fluorescent cells if samples were maintained at 200×10^{-6} mol/L O_2 for 30 minutes. Furthermore, on cessation of hypoxia, fluorescence rapidly increased toward prehypoxic levels (data not shown). This effect of hypoxia on O_2 consumption did not occur following treatment with L-NA (Figure 3A and 3B and Online Movies), indicating that it was NO-dependent and that an active NO synthase was generating NO at concentrations sufficient to modulate the consumption of O_2 ¹⁴ and divert it toward the surrounding tissues. This is supported by the fact that sodium cyanide, which also inhibits the CcO, produced a similar increase in the concentration of O_2 in the cells (see Online Movies).

Treatment with ACh further increased the build up of O_2 in hypoxia and the speed at which it occurred (Figure 3A and 3B and Online Movies). Thus, on induction of hypoxia, it took 6.40 ± 0.2 minutes to reduce by 50% the number of control fluorescent cells and only 5.20 ± 0.3 minutes in the presence of ACh. Administration of the same dose of ACh at 200×10^{-6} mol/L O_2 also elicited a decrease in ruthenium fluorescence that was smaller than that observed in hypoxia but was still significant (Figure 4A and 4B and Online Movies). This response was substantially enhanced if hypoxia was induced subsequently. Treatment with L-NA prevented the effects of ACh (Figure 4B) but had no effect on the similar response induced by DETA-NO (1×10^{-5} mol/L) (data not shown). Experiments in eNOS knockout mice further showed that, whereas mesenteric tissues from WT mice exhibited a similar NO-dependent increase in the concentration of tissue O_2 to that obtained in rats, those from eNOS knockout animals showed no changes in fluorescence during hypoxia (Figure 3A and 3C and Online Movies), even after the administration of ACh (data not shown).

Discussion

Our results indicate that both basal and stimulated release of NO from the vascular endothelium is responsible not only for the well-known regulation of vascular tone¹ but also for the adjustment of O_2 consumption. In our experiments using isolated blood vessels, although we studied the consumption of O_2 over a wide range of $[O_2]$, we chose to compare the behavior of the vessels at 2 $[O_2]$, namely 130×10^{-6} mol/L and 30×10^{-6} mol/L, which approximate the $[O_2]$ in arterial blood and tissues, respectively. Our results demonstrate that as the $[O_2]$ decreased so did the consumption of O_2 . In the absence of endothelium-derived NO, following inhibition of its synthesis with L-NA or removal of the endothelium, this adaptive change disappeared and the vascular consumption of O_2 remained constant over a wide range of $[O_2]$. There was eventually a drop in consumption in the absence of NO; however, this occurred at much lower $[O_2]$.

This modulatory effect of NO was observed in a variety of vessels of different anatomic origin and sources, including human, and is consistent with its known effect in reducing the

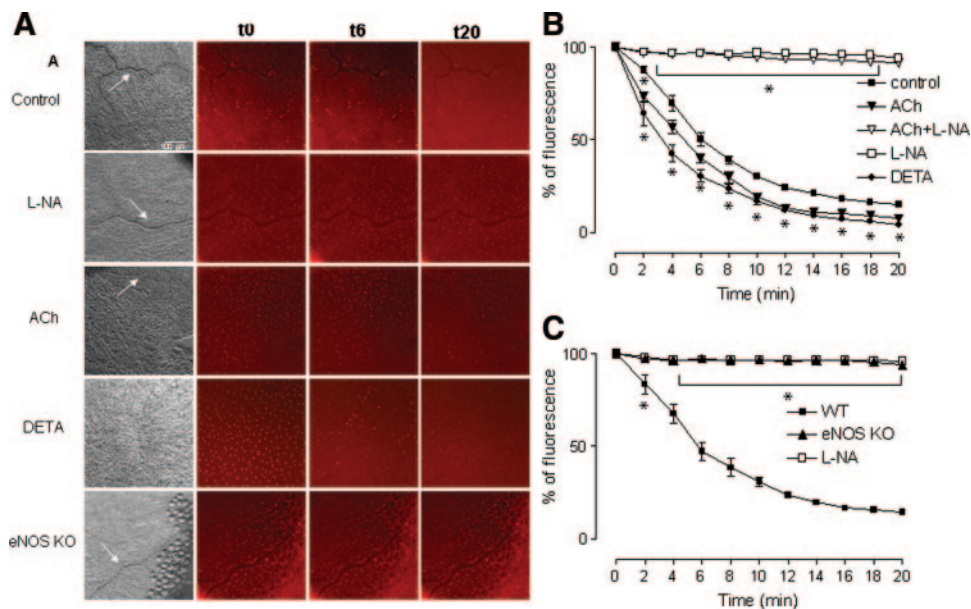


Figure 3. Changes in intracellular $[O_2]$ in rat and mice mesenteric cells, in close proximity to a blood vessel, when exposed to hypoxia. The preparation was loaded with $Ru(phen)_3^{2+}$ (3 hours, 1×10^{-4} mol/L, red fluorescence), whose fluorescence is inversely proportional to the $[O_2]$. Following a 10-minute equilibration period at atmospheric $[O_2]$ (200×10^{-6} mol/L O_2), samples were subjected to hypoxia (15×10^{-6} mol/L O_2) for a 20-minute period by the addition of nitrogen in the presence or absence of L-NA (1×10^{-4} mol/L), ACh (1×10^{-5} mol/L), or DETA-NO (1×10^{-5} mol/L). Fluorescence in individual cells was monitored at 2 minutes intervals following hypoxia, as shown in A, where phase-contrast images of the selected area are shown (left), and the arrows show the blood vessels. B and C show the changes in $Ru(phen)_3^{2+}$ fluorescence intensity expressed as a percentage of basal fluorescence. Data are means \pm SEM from 5 independent experiments and $*P < 0.05$ vs value at 200×10^{-6} mol/L O_2 (time 0). Bar = 100 μm .

affinity of CcO for O_2 in a competitive manner, ie, increasing its K_m and adjusting mitochondrial O_2 consumption.^{8,15} We found that aortas from eNOS knockout mice exhibited a reduced K_m for O_2 and consumed equal amounts of O_2 independently of the $[O_2]$ in the medium, further indicating

that endothelium-derived NO is responsible for regulating O_2 consumption.

When endothelial NO generation was increased with ACh or Bk, at concentrations at which these agonists produced potent sGC-mediated vasodilation,¹⁶ there was an enhanced reduction in V_{O_2} . This occurred even at the higher $[O_2]$ and was also prevented by treatment with L-NA or removal of the endothelium. Administration of exogenous NO with DETA-NO also induced a greater inhibition of O_2 consumption and increase in K_m , which were not affected either by inhibition of NO generation or by removal of the endothelium. These results are in accordance with previous observations in cells^{3,9} and in tissues.^{4,7,17} This NO-dependent effect on consumption of O_2 was also observed in the presence of the vasoconstrictor Phe, which is known to release NO following activation of endothelial α_1 adrenoreceptors.¹⁸

Inhibition of CcO by NO (a phenomenon that has been called "metabolic hypoxia"¹⁸) leads to a major redistribution of O_2 , which has been demonstrated in cells in culture.^{6,19} Our results, obtained with fluorescence microscopy show that this redistribution also occurs in vascular tissues in vitro. Indeed, these experiments show that the stimulation of endothelial NO production with ACh resulted in an increase in the intracellular $[O_2]$ of the mesenteric cells surrounding a microvessel, as shown by the decreased fluorescence of $Ru(phen)_3^{2+}$. This effect could be observed even in experiments carried out at 200×10^{-6} mol/L O_2 , in which ACh was able to generate enough NO to modulate O_2 consumption. Addition of DETA-NO and other inhibitors of mitochondrial respiration to the vascular preparations also led to an increase in the intracellular $[O_2]$, indicating a concentration-dependent

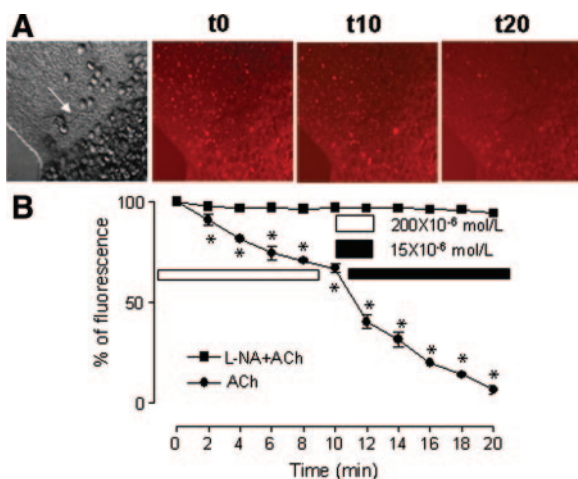


Figure 4. Effect of ACh on intracellular $[O_2]$ in rat mesenteric cells, in close proximity to a blood vessel. The preparation was loaded with $Ru(phen)_3^{2+}$, as described in the legend to Figure 3. Following 10 minutes of equilibration at 200×10^{-6} mol/L O_2 , ACh (1×10^{-5} mol/L) was added for a further 10 minutes, and samples were then subjected to hypoxia (15×10^{-6} mol/L O_2) for 10 minutes in the presence or absence of L-NA (1×10^{-4} mol/L). Fluorescence in individual cells was monitored at 2-minute intervals, as shown in A and B. B shows the changes in $Ru(phen)_3^{2+}$ fluorescence intensity expressed as a percentage of basal fluorescence. Data are means \pm SEM from 5 independent experiments and $*P < 0.05$ vs value at 200×10^{-6} mol/L O_2 .

effect of NO. The reason for the paradoxical increase in cellular $[O_2]$ when exposed to hypoxia is that in normoxia, where O_2 consumption is high, there is a steep O_2 gradient toward O_2 -consuming mitochondria, leaving a relatively low level of spare O_2 (hence high ruthenium fluorescence). In hypoxia, NO-dependent inhibition of respiration leads to decreased O_2 consumption and thus a paradoxical increase in the levels of available O_2 (hence a lower number of ruthenium fluorescent cells).

In conclusion, our results indicate that the basal release of endothelial NO adjusts vascular O_2 consumption. This may occur at the level of the microcirculation to facilitate the distribution of O_2 to the tissues, especially at low $[O_2]$, as has been indicated before.^{6,20,21} It may also occur in the larger vessels, where the requirement for O_2 by the vascular smooth muscle may vary as a result of the action of hormones such as ACh and adrenaline, as well as the activity of the different sets of nerves that innervate the vasculature. This remains to be studied. In addition, it is possible that changes in the distribution of O_2 throughout the vessel wall, because of a decrease in NO production in endothelial dysfunction, may play a role in the development of vascular disease.

Acknowledgments

We thank Annie Higgs and Brian Normanly for help with manuscript preparation and Eoin Cummins for assistance with imaging.

Sources of Funding

This study was supported by Ministerio de Educación y Ciencia (Spain) grant PI07/0091 and Contrato-Investigador Fondo de Investigación Sanitaria (FIS) grant CP07/00171 (to V.M.V.). J.V.E. is the recipient of Ministerio de Educación y Ciencia (Spain) grants SAF 2005-01366 and PI08/1325, and P.D. is the recipient of Ministerio de Educación y Ciencia (Spain) grant SAF 2004-01541. C.T.T. is the recipient of a grant from the Science Foundation Ireland. S.M. is supported in part by the European FP6 (LSHM-CT-2004-0050333).

Disclosures

None.

References

- Moncada S, Higgs EA. The discovery of nitric oxide and its role in vascular biology. *Br J Pharmacol*. 2006;147:193–201.
- Galkin A, Higgs A, Moncada S. Nitric oxide and hypoxia. *Essays Biochem*. 2007;43:29–42.
- Clementi E, Brown GC, Foxwell N, Moncada S. On the mechanism by which vascular endothelial cells regulate their oxygen consumption. *Proc Natl Acad Sci U S A*. 1999;96:1559–1562.
- Loke KE, McConnell PI, Tuzman JM, Shesely EG, Smith CJ, Stackpole CJ, Thompson CI, Kaley G, Wolin MS, Hintze TH. Endogenous endothelial nitric oxide synthase-derived nitric oxide is a physiological regulator of myocardial oxygen consumption. *Circ Res*. 1999;84:840–845.
- Walsh EK, Huang H, Wang Z, Williams J, de Crom R, van Haperen R, Thompson CI, Lefer DJ, Hintze TH. Control of myocardial oxygen consumption in transgenic mice overexpressing vascular eNOS. *Am J Physiol Heart Circ Physiol*. 2004;287:2115–2121.
- Hagen T, Taylor CT, Lam F, Moncada S. Redistribution of intracellular oxygen in hypoxia by nitric oxide: effect on HIF1 α . *Science*. 2003;302:1975–1978.
- Núñez C, Victor VM, Tur R, Alvarez-Barrientos A, Moncada S, Esplugues JV, D'Ocon P. Discrepancies between nitroglycerin and NO-releasing drugs on mitochondrial oxygen consumption, vasoactivity, and the release of NO. *Circ Res*. 2005;97:1063–1069.
- Moncada S, Erusalimsky JD. Does nitric oxide modulate mitochondrial energy generation and apoptosis? *Nat Rev Mol Cell Biol*. 2002;3:214–220.
- Palacios-Callender M, Quintero M, Hollis VS, Springett RJ, Moncada S. Endogenous NO regulates superoxide production at low oxygen concentrations by modifying the redox state of cytochrome c oxidase. *Proc Natl Acad Sci U S A*. 2004;101:7630–7635.
- Esplugues JV, Rocha M, Nuñez C, Bosca I, Ibiza S, Herance JR, Ortega A, Serrador JM, D'Ocon P, Victor VM. Complex I dysfunction and tolerance to nitroglycerin: an approach based on mitochondrial-targeted antioxidants. *Circ Res*. 2006;99:1067–1075.
- Paxian M, Keller SA, Cross B, Huynh TT, Clemens MG. High-resolution visualization of oxygen distribution in the liver in vivo. *Am J Physiol Gastrointest Liver Physiol*. 2004;286:37–44.
- Asiedu JK, Ji J, Nguyen M, Rosenzweig N, Rosenzweig Z. Development of a digital fluorescence sensing technique to monitor the response of macrophages to external hypoxia. *J Biomed Opt*. 2001;6:116–121.
- O'Neal DP, Pishko M, Meledeo A, Ibey B, Gant A, Davis J, Coté GL. Oxygen sensor based on the fluorescence quenching of a ruthenium complex immobilized in a biocompatible poly(ethylene glycol) hydrogel. *IEEE Sensors J*. 2004;4:1–7.
- Palacios-Callender M, Hollis V, Mitchinson M, Frakich N, Unitt D, Moncada S. Cytochrome c oxidase regulates endogenous nitric oxide availability in respiring cells: a possible explanation for hypoxic vasodilation. *Proc Natl Acad Sci U S A*. 2007;104:18508–18513.
- Brown GC, Cooper CE. Nanomolar concentrations of nitric oxide reversibly inhibit synaptosomal respiration by competing with oxygen at cytochrome oxidase. *FEBS Lett*. 1994;356:295–298.
- Garland CJ, Plane F, Kemp BK, Cocks TM. Endothelium-dependent hyperpolarization: a role in the control of vascular tone. *Trends Pharmacol Sci*. 1995;16:23–30.
- Zhao X, He G, Chen YR, Pandian RP, Kuppusamy P, Zweier JL. Endothelium-derived nitric oxide regulates postischemic myocardial oxygenation and oxygen consumption by modulation of mitochondrial electron transport. *Circulation*. 2005;111:2966–2972.
- Tuttle JL, Falcone JC. Nitric oxide release during α 1-adrenoreceptor-mediated constriction of arterioles. *Am J Physiol Heart Circ Physiol*. 2001;281:873–881.
- Quintero M, Colombo SL, Godfrey A, Moncada S. Mitochondria as signaling organelles in the vascular endothelium. *Proc Natl Acad Sci U S A*. 2006;103:5379–5384.
- Poderoso JJ, Carreras MC, Lisdero C, Riobo N, Schopfer F, Boveris A. Nitric oxide inhibits electron transfer and increases superoxide radical production in rat heart mitochondria and submitochondrial particles. *Arch Biochem Biophys*. 1996;328:85–92.
- Thomas DD, Liu X, Kantrow SP, Lancaster JR. The biological lifetime of nitric oxide: implications for the perivascular dynamics of NO and O_2 . *Proc Natl Acad Sci U S A*. 2001;98:355–360.

Supplement Material

Legend for supplementary films.

Hypoxia-induced changes in intracellular $[O_2]$ in rat and mouse mesenteric cells in close proximity to a blood vessel. The preparation was loaded with $Ru(phen)_3^{2+}$ (3h, 1×10^{-4} mol/L μM , red fluorescence), whose fluorescence is inversely proportional to the $[O_2]$. Fluorescence was filmed for a 20 min period in normoxia or hypoxia, recording one frame every 2 min. When tissues were subjected to hypoxia following normoxia, the first frame was taken in normoxia and the subsequent frames in hypoxia. (A) Control normoxia, (B) control hypoxia, (C) hypoxia in the presence of L-NA, (D) hypoxia in the presence of ACh, (E) hypoxia in the presence of DETA-NO, (F) normoxia in the presence of cyanide, (G) hypoxia in cells from eNOS^{-/-} mice, (H) addition of ACh in the presence of normoxia, and (I) hypoxia in the presence of ACh.

Online Figure I.

Representative images of cells from the mesenterium showing the changes that took place in intracellular $[O_2]$ when exposed to hypoxia (nucleus stained with Hoescht (blue), O_2 stained with $Ru(phen)_3^{2+}$ (red) in the cytosol of the cells). The preparation was loaded with $Ru(phen)_3^{2+}$ (3h, 1×10^{-4} mol/L, red fluorescence), whose fluorescence is inversely proportional to the $[O_2]$. The vital cell nuclear stain Hoechst 33342 (1×10^{-6} mol/L) was added for the last 30 min of incubation. Following a 10 min equilibration period at atmospheric $[O_2]$ (200×10^{-6} mol/L O_2), samples were subjected to hypoxia (15×10^{-6} mol/L O_2) for a 20 min period by the

addition of nitrogen. The panels on the left show the merged fluorescence of Hoescht (blue) and Ru(phen)_3^{2+} (red) while the panels on the right show Ru(phen)_3^{2+} alone.

Online Figure I

